Interface Engineering of Noble-Metal-Free 2D Cu-MoS_2 Nanocomposites for Enhanced Photocatalytic Analysis

Arti[1], Naushad Alam[1*], Jamilur R. Ansari[2*]

[1]Department of Physics, Lalit Narayan Mithila University, Darbhanga-846004, Bihar, India
E-mail: *kumariarti0079[at]gmail.com*
[2]Department of Applied Science, Laxmi Devi Institute of Engineering & Technology,
Chikani, Alwar-301028, Rajasthan, India

***Corresponding Authors**
Professor Naushad Alam, E-mail: nalam8841[at]gmail.com
Professor Jamilur R. Ansari, E-mail: drjransari1[at]gmail.com

Abstract: ***Molybdenum disulfide popularly known as MoS_2, a remarkable 2D transition metal, incorporated with Copper (Cu) nanocomposites emerged as a significant nanocomposite material which enhances its optical, electrical and catalytic properties. The synergistic ability of Cu-MoS_2 nanocomposites also improves the stability, charge transfer ability as well as catalytic efficiency. The remarkable properties like tunable band gap, effective mechanical strength and larger surface area provided by MoS_2 governed its application in energy storage, photocatalysis and sensing. The synergistic incorporation of MoS_2 nanosheets with noble metal like Cu not only enhances its performance but also leads to its application in various fields. Here a solvothermal process is used to synthesize Cu-MoS_2 nanocomposites. The analysis of the morphology of Cu-MoS_2 and its various characteristics can be governed through the study of photoluminescence (PL) spectra, UV-Vis spectroscopy, X-ray photoelectron spectroscopy (XPS), high-resolution transmission electron microscopy (HRTEM) and Fourier-transform infrared spectroscopy (FTIR). The degradation efficiency of Cu and Cu-MoS_2 nanocomposite comprises of 41% and 81% as demonstrated from photocatalytic degradation experiment consisting of a solution of 5μM methylene blue concentration. It upgrades the potential of Cu-MoS_2 nanocomposite in photocatalytic degradation application.***

Keywords: Molybdenum disulfide, nanocomposites, copper, methylene blue, electrocatalysis, degradation.

1. Introduction

This work focuses on the synthesis of high-purity MoS_2, Cu, and Cu-MoS_2 nanocomposite using both ultrasonication and sol-gel methods. The resulting MoS_2, Cu, and Cu-MoS_2 nanocomposites were meticulously examined for their photocatalytic properties, particularly in the degradation of Methylene Blue dye. A significant highlight of this research is the successful creation of novel Cu-MoS_2 nanocomposites synthesized through the solvothermal process. The photocatalytic performance of this innovative catalyst was rigorously tested for the breakdown of organic dyes, specifically Methylene Blue (MB), under ultraviolet light exposure. The samples were subjected to irradiation for up to 45 minutes using direct solar energy, showcasing the potential of this approach in developing photocatalysts aimed at addressing water pollution challenges[1–3]. A diverse array of semiconductor materials has been thoroughly explored for their potential in energy production and environmental remediation[4–6]. Among these, Copper (Cu) emerging as a particularly compelling candidate due to its remarkable properties. With a large band gap of approximately 3.37 eV, high exciton binding energy, nontoxicity, and excellent electron mobility, coupled with its abundance in nature, Cu has garnered extensive attention in recent research endeavors[7–9]; however there is some limitations in the absorbing capacity of solar spectrum of the Cu nanoparticles; it can only capture about 5% of the total solar energy in the ultraviolet (UV) region due to its substantial band gap energy. High-resolution transmission electron microscopy (HRTEM) analyses have illuminated the intricate morphology as well as the dimensions of synthesized MoS_2, Cu, and Cu-MoS_2 nanocomposites, revealing that they are composed of nanorods expertly coated with MoS_2. Furthermore, the results of photocatalytic degradation experiments demonstrate that the as-synthesized Cu and Cu-MoS_2 nanocomposites exhibit impressive degradation efficiency of 41% and 81%, respectively, when treating a 5 μM methylene blue (MB) solution. Cu, recognized as an n-type semiconductor due to its wide band gap and ease of synthesis, stands out for its economical fabrication methods and exceptional performance in the UV spectrum, reinforcing its status as a highly effective photocatalytic agent[10–12].

This study details the successful fabrication of Cu-MoS_2 nanocomposites as a photocatalyst, prepared through a solvothermal synthesis approach[13]. The evaluation of photocatalytic phenomenon regarding the methylene blue degradation applying UV radiation was done, with exposure times extending to 60 minutes. The maximum absorbance for MB was detected at 660 nm, and the degradation kinetics were characterized by first-order behavior[14,15]. The creation of Cu-MoS_2 nanocomposites as heterojunctions remarkably boosted photocatalytic performance by effectively promoting the separation of charge carriers, which in turn led to enhanced efficiency. A comprehensive exploration of the photocatalytic mechanism illuminated the essential roles played by photo generated holes and hydroxyl radicals in the degradation process, highlighting their critical contributions to the overall reaction dynamics [16–18].

This research presents an innovative strategy for the development of bi-functional photocatalysts specifically designed to address the critical issue of water pollution. Cu remains a material of significant interest in this field due to its wide band gap of approximately 3.37 eV, which allows for effective charge separation and enhanced photocatalytic activity. Its advantageous properties facilitate both energy conversion processes and environmental remediation efforts. However, it is important to note that Cu's solar absorption capabilities are primarily confined to the ultraviolet spectrum (wavelengths below 400 nm), which poses challenges for its application under visible light conditions. This study explores various modifications and enhancements to Cu, aiming to broaden its absorption spectrum and improve its photocatalytic efficiency in degrading pollutants in water systems. By leveraging advanced synthesis techniques and composite material approaches, this research seeks to optimize the performance of Cu-based photocatalysts, ultimately contributing to cleaner water solutions [19, 20].

2. Synthesis Materials

Copper Sulfate powder, ethyl alcohol, deionized water, sodium hydroxide (NaOH) ammonium tetrathiomolybdate [$(NH_4)_2$ MoS_4], hydrazine (N_2H_4), Methylene Blue (MB),

2.1 Synthesis of Cu Nanorods

In this synthesis process, 0.015 moles of Cu sulfate powder were carefully dissolved in 10 mL of a concentrated 10 mol/L NaOH solution. To this mixture, 490 mL of water was added, creating a homogenous solution. The resulting mixture was subjected to microwave irradiation, where it was heated to a precise temperature of 600°C for 20 minutes. Following this heating phase, the solution was allowed to cool, and a white precipitate formed, which was subsequently collected through filtration. Distilled water and ethanol are used to wash the precipitate to ensure purity, resulting in a refined final product[6,10].

2.2 Synthesis of MoS_2 nanosheets

In this experimental procedure, 0.05 grams of ammonium tetrathiomolybdate [$(NH4)_2MoS_4$] powder was carefully dispersed in a well-stirred solution having 10 ml of ethanol mixed with 10 ml of distilled water, maintaining a constant stirring for one hour to ensure uniform distribution. Following this, 1 ml of hydrazine hydrate (N_2H_4) was gradually introduced into the solution, initiating a chemical reaction. For enhancing the dispersion of the materials, the mixture was subjected to sonication for an impressive duration of 10 hours in an ultrasonic bath, which helped to break down the aggregates and produce fine MoS_2 sheets. After sonication, the resultant dispersion was centrifuged at 3000 rpm for 10 minutes to facilitate the purification of the MoS_2 sheets[21–23]. The purified product was then carefully dispersed in 30 ml of ethanol, preparing it for subsequent characterization.

2.3 Synthesis of Cu-MoS_2 nanocomposites

A specific quantity of molybdenum disulfide was meticulously incorporated into a 300 mL suspension of ethanol, which included 0.5 g of CuNPs. This mixture was subjected to continuous stirring for 24 hours to ensure thorough dispersion and interaction between the components. Afterward, the combined solution underwent centrifugation at a speed of 2000 rpm to separate the solid particles from the liquid phase. The resulting precipitate was subsequently washed multiple times with ethanol to remove any unreacted materials and impurities. The final product was then dried overnight under a temperature of 60°C in an oven to eliminate residual solvent and consolidate the heterojunction structure. This naming convention reflects the precise ratio of MoS_2 incorporated within the Cu matrix, which is expected to influence the heterojunction's properties and potential applications in various fields, such as photocatalysis, optoelectronics, and energy storage.

3. Results and Discussion

3.1 PL analysis of Cu-MoS_2 nanocomposites

The photoluminescence (PL) spectrum of Cu-MoS_2 nanocomposite provides valuable information about its electronic structure, excitonic recombination and charge transfer behavior. Figure 1 depicts strong PL emission of the pristine MoS_2 semiconductor. Some modification occurs in the PL spectrum due to the incorporation of Cu nanoparticles. This is because of charge transfer interactions, exciton quenching and defect state formation. Here the excitation peaks of MoS_2 are significantly attenuated due to the presence of Cu, which result in the form of transfer of electron from photo excited MoS_2 to Cu. The incorporation of Cu metal introduces additional pathway in case of non- radiative recombination, which reduces overall PL intensity. The quenching extent is governed by the particle size, dispersion as well as the interaction strength between Cu and MoS_2.

The **Figure 1** depicts a sharp peak at 805 nm. This peak is the indicator of excitonic transition which is governed by the band structure due to Cu-MoS_2 interactions. This also reflects the optical properties of MoS_2, which is the result of charge transfer effects of Cu or localized surface plasmon resonance (LSPR) of Cu nanoparticles. The other region of the spectrum does not show any other peak at any wavelength which confirms the dominance of 805 nm peak in the PL response.

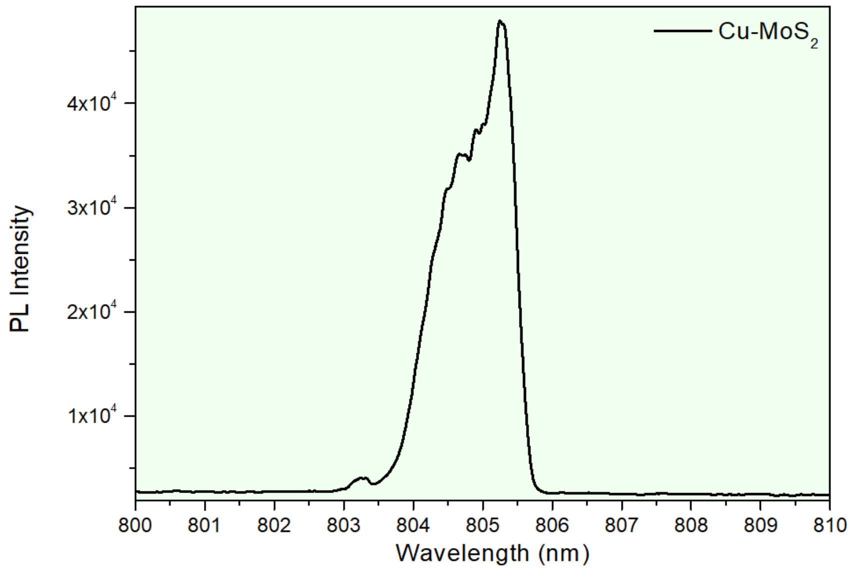

Figure 1: PL spectra of synthesized Cu-MoS_2 nanocomposite

3.2 UV Vis spectra analysis of Cu-MoS_2 nanocomposites

The UV-vis spectra of MoS_2nanoflakes as well as the Cu-MoS_2 nanocomposites are illustrated in **Figure 2**, spanning the wavelength range of 300 to 700 nm. Notably, the MoS_2/Cu nanocomposites exhibited significantly enhanced light absorption compared to the individual components. This result underscores the impact of integrating Cu with MoS_2 into the Cu-MoS_2 nanocomposites, markedly improving its light-harvesting capabilities. Pure Cu, characterized by an absorption edge around 365 nm, demonstrated substantial absorption primarily within the ultraviolet (UV) region, indicating its potential for UV-driven applications. In contrast, the Cu-MoS_2 nanocomposites, which displayed distinctive orange hues, exhibited significantly greater absorbing capacity in the visible light spectrum as compared to the weak blue absorption of pure Cu.

This enhanced absorption capacity in the visible region can be attributed to the introduction of MoS_2, which facilitates a broader light absorption profile. Moreover, the incorporation of MoS_2 nanoparticles into the Cu matrix enabled the nanocomposites to absorb light effectively across the entire UV/Vis range (200-800 nm). This comprehensive absorption spectrum not only improves the photocatalytic properties of the material but also highlights the synergistic interactions between MoS_2 and Cu, making Cu-MoS_2 nanocomposite promising candidates for various optoelectronic and photocatalytic applications[11,24].

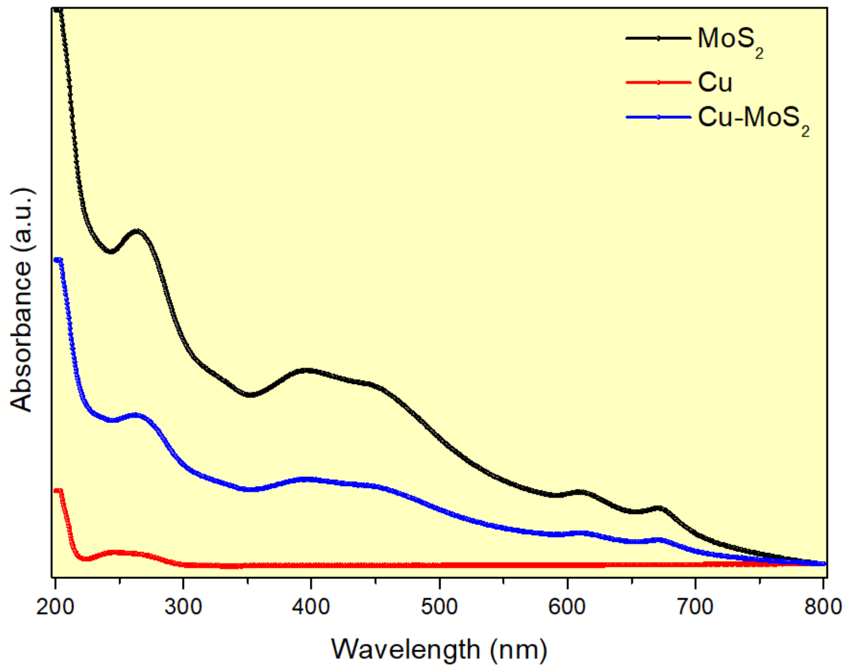

Figure 2: UV-Vis spectra of MoS_2 nanosheets, Cu NPs and Cu-MoS_2 nanocomposite

3.3 TEM analysis of Cu-MoS_2 nanocomposites

We conducted a detailed investigation into the microstructure of the synthesized samples. The vertically aligned Cu nanorods (NRs) are illustrated in **Figure 3(a-d)**, which include selected area electron diffraction (SAED) and transmission electron microscopy (TEM) images, respectively. Our analysis revealed that the average side-to-side diameter of the nanorods is approximately 124.7 nanometers.

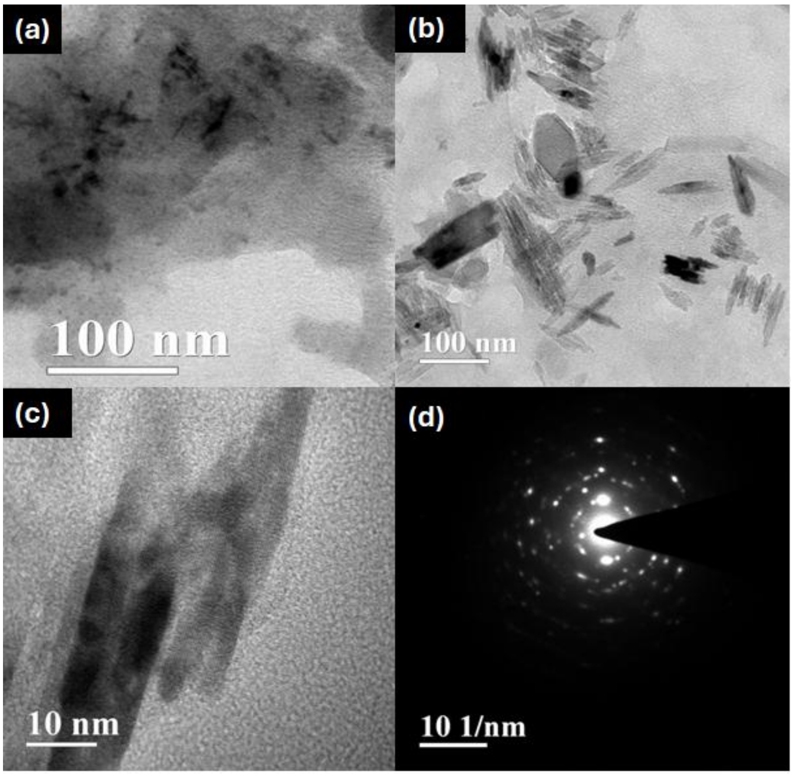

Figure 3: (a-b) TEM (c) HRTEM and (d) SAED image of Cu-MoS_2 nanocomposite

Utilizing the X-ray diffraction (XRD) data presented previously in the figures, we identified an interplanar spacing of 0.26 nanometers from high-resolution TEM imagery, which can be attributed to the (002) plane of Cu. However, further analysis depicted that these nanoparticles (NPs) are likely composed of Cu NPs coated with multiple layers of molybdenum disulfide (MoS_2) nanosheets. Previous literature indicates that under optimal conditions, specifically regarding the concentration of the sulfur precursor and the duration of the reaction, the outer layer of Cu NRs can undergo a transformation to Cu_2S. Despite several Cu NRs maintaining their characteristic hexagonal rod shape, we can observe signs of partial conversion from Cu to Cu_2S. In our experimental setup, the transformation is driven by the interaction of sulfur derived from CH_3CSNH_2 with the Cu NRs. Moreover, there is additional sulfur present that interacts with sodium molybdate dihydrate ($Na_2MoO_4{\cdot}2H_2O$), facilitating the formation of low-density MoS_2 nanosheets [21,25,26]. To create Cu-MoS_2 nanocomposites, these few-layer MoS_2 nanosheets aggregate and envelop the outer layers of the composite. The high-resolution TEM images provide compelling evidence of the two distinct phases-Cu, and MoS_2 by displaying three separate lattice fringes. Specifically, the interlayer spacing of 0.69 nanometers is consistent with the (002) plane of MoS_2, while interlayer spacing of 0.32 nanometers and 0.26 nanometers correspond to the (111) facets of Cu_2S and the (002) plane of Cu, respectively. These measurements correlate well with our findings from the crystallographic analysis, further confirming the structural integrity and morphological attributes of the synthesized nanocomposites.

3.4 FTIR analysis of Cu-MoS_2 nanocomposites

For investigating the presence of functional groups and metallic bonds, Fourier Transform Infrared (FTIR) spectroscopy analyses were conducted over a wave number range of 400 to 4000 cm^{-1} at ambient temperature. The spectra for Cu, molybdenum disulfide (MoS_2), and the composite Cu-MoS_2 are presented in **Figure 4**. The results confirm the formation of metal-oxygen bonds within both Cu and MoS_2. Prominent peaks at approximately 1012 cm^{-1} and 1310 cm^{-1} correspond to the Cu-O bond and the Mo-S bond, respectively.

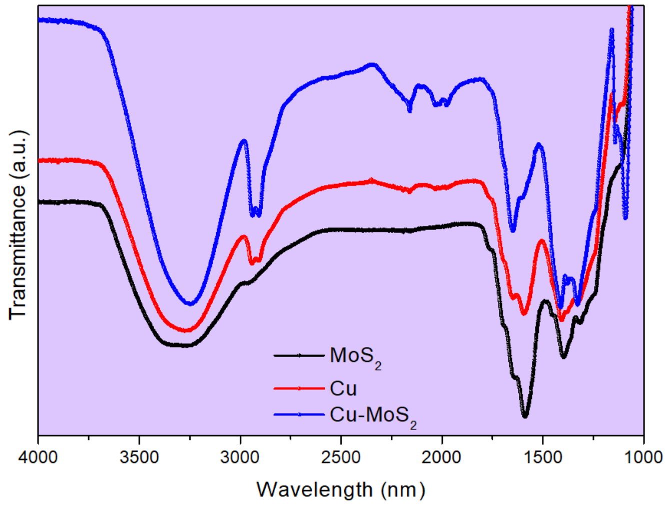

Figure 4: FTIR spectra of MoS_2 nanosheets, Cu NPs and Cu-MoS_2 nanocomposite

Additionally, a broad peak near 1648 cm^{-1} indicates the availability of hydrogen-oxygen bonds, likely sourced from the ambient moisture. For Cu, strong absorption bands are observed at approximately 3400 cm^{-1},1550 cm^{-1}, and 1463.36 cm^{-1}, which are attributed to O–H stretching, H–O–H bending vibrations, and Cu–O stretching vibrations, respectively[27,28]. In the case of MoS_2, a distinct peak at around 1135 cm^{-1} is attributed to S-S bond vibrations, while a peak at approximately 469 cm^{-1} corresponds to Mo-S stretching vibrations. Notably, both Cu and MoS_2 exhibit a significant absorption band near 3440 cm^{-1}, which is linked to O–H and H–O–H stretching vibrations, further highlighting interactions with moisture. This comprehensive spectral analysis underscores the distinct bonding characteristics and the potential interactions occurring within the materials under investigation.

3.5 XPS analysis of Cu-MoS2 nanocomposites

In X-ray Photoelectron Spectroscopy (XPS), the analysis comprises the availability of multiple components acting as photocatalysts within the sample. According to the literature, **Figure 5 (a-d)** illustrates the comprehensive survey of Cu alongside high-resolution scans of the Mo3d, Cu 2p, and S2p peaks, along with their optimal deconvolution into individual components. Notably, in the MoS_2 3d spectra, two distinct peaks corresponding to the Mo $3d_{3/2}$ and Mo $3d_{5/2}$ states were identified at 229.2 eV and 232.8 eV, respectively. These energy levels confirm the oxidation states of molybdenum within the MoS_2 . Furthermore, because the MoS_2 lattice does not alter the chemical makeup of the Cu nanoparticles, the two peaks observed in the O1s spectra at 332.6 eV and 331.3 eV can be attributed, respectively, to the oxygen functionalities associated with the organic linkers in the structure and the Cu lattice oxygen bonded to the Cu nanoparticles.

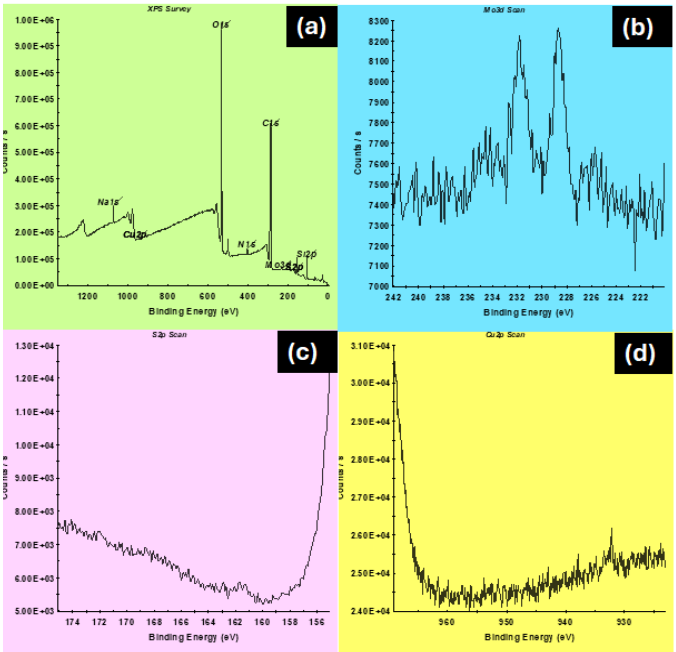

Figure 5: XPS Analysis of Cu-MoS_2 nanocomposites (a) Survey (b) MoS_2 (c) S2p and (d) Cu NPs

Additionally, the presence of nitrogen (N) and sulfur (S) dopants on the surface of the MoS_2 was conclusively demonstrated through the XPS analysis. The high-resolution N1s spectrum reveals a peak at 401.1 eV, distinctly indicating the presence of MoS_2-N bonds, which suggests the incorporation of nitrogen into the MoS_2 framework. Moreover, in the high-resolution S2p spectrum, a prominent single peak at a binding energy of 161.8 eV was observed. This peak is attributed to carbon-sulfur (CS) bonding, further supporting the presence of sulfur functionalities incorporated within the MoS_2 matrix, as deduced from the extensive characterization data acquired during the study. This comprehensive analysis establishes a clearer understanding of the electronic environment and bonding characteristics within the investigational materials[12,17,29].

3.6 Photocatalytic Analysis of Cu-MoS_2 Nanocomposites

To effectively degrade the dye, a Cu-MoS_2 nanocomposite was employed as a photocatalytic semiconductor under a light source of energy. The analysis of the absorbance versus wavelength graph indicates that the degradation efficiency of the Cu-MoS_2 nanocomposites surpasses that of individual Cu and MoS_2 components. Specifically, the Cu-MoS_2 nanocomposites governed an impressive dye degradation rate of up to 90% within just 60 minutes, as illustrated in the corresponding graph. In this study, we utilized as-synthesized MoS_2, Cu, and Cu-MoS_2 nanocomposites as photocatalysts for the degradation of Methylene Blue (MB). **Figure 6(a)** presents the UV-Vis absorption spectra for investigating the photocatalytic degradation of a 5 μM MB solution[30,31]. These samples were irradiated with direct solar energy for 60 minutes, allowing us to monitor the degradation process effectively. The characteristic absorption peak for MB was observed at 660 nm, and this peak intensity was tracked as a function of exposure time to solar energy. The kinetics of the photocatalytic degradation of MB dyes with the Cu and Cu-MoS_2 nanocomposite conform to first-order kinetics, as demonstrated in **Figure 6(b).** The results show that the as-prepared Cu and Cu-MoS_2 nanocomposites facilitated photocatalytic degradation of 41% and 81% of the 5 μM MB solutions, respectively, as illustrated in **Figure 6(c).** The calculated rate constants for the degradation processes were determined to be 29.1×10^{-3} min^{-1} for Cu and 74.1×10^{-3} min^{-1} for the Cu-MoS_2 nanocomposite. Additionally, we evaluated the recyclability and eco-friendly characteristics of both Cu as well as Cu-MoS_2 photocatalysts by performing multiple degradation cycles with the same samples, repeating the reactions three times, as presented in **Figure 6(d).** The synthesized Cu-MoS_2 nanocomposites show great potential for practical photocatalytic applications, demonstrating not only high efficiency but also sustainability in environmental remediation efforts [32,33].

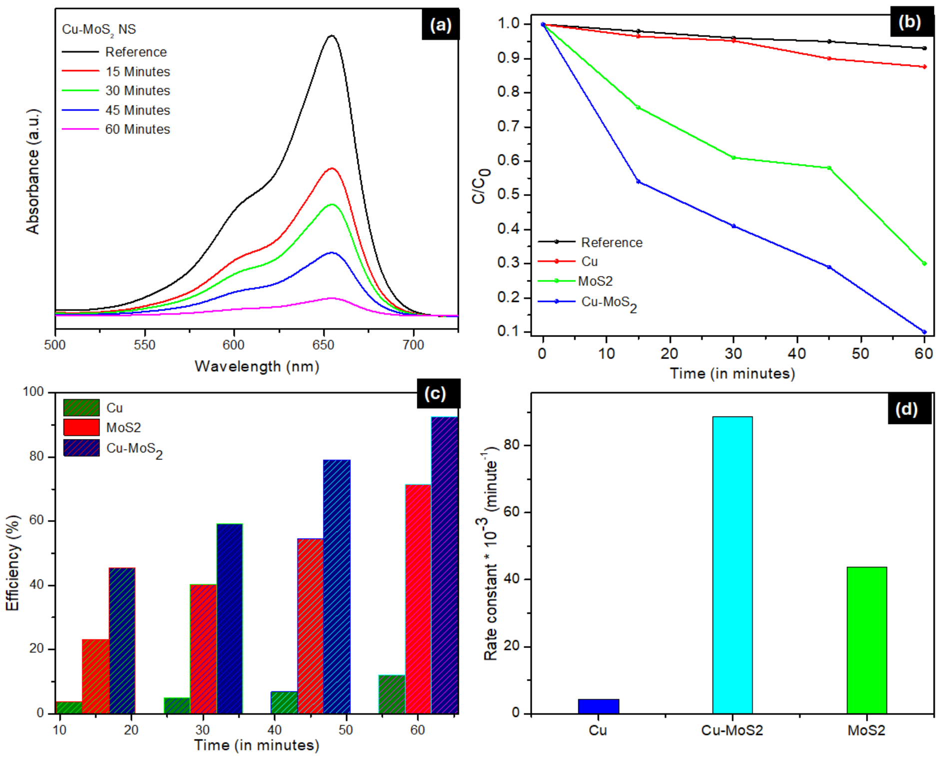

Figure 6: (a) UV-Vis absorption spectra for photocatalytic degradation of 5 μM for the degradation of Methylene Blue (MB) for the synthesized materials (b) Rate Constant (c) Efficiency and (d) Reusability of Cu-MoS_2 nanocomposites

4. Conclusion

The Cu-MoS_2 nanocomposites have been successfully synthesized, marking a significant advancement in composite material development. The X-ray diffraction (XRD) pattern distinctly confirmed the crystal structure and average particle size of the composite, indicating a well-defined arrangement at the atomic level. Furthermore, the UV-visible spectroscopy of MoS_2sheets and the Cu-MoS_2 nanocomposites illustrated a broad absorption capacity spanning the entire ultraviolet to visible spectrum (200-800 nm), showcasing their potential for light-harvesting applications. The Raman spectrum of the Cu-MoS_2 nanocomposite revealed the presence of pure phases of both MoS_2 and Cu, effectively validating the findings from the XRD analysis. High-resolution transmission electron microscopy (TEM) images portrayed the nanoparticles as being well within the nanoscale range, characterized by a uniform formation of hexagonal nanorods. Remarkably, the average diameter across the hexagonal nanorods measured 124.7 nm, emphasizing their consistent architectural design. The polycrystalline nature of the Cu-MoS_2 nanocomposite was further corroborated through high-resolution TEM imaging, which revealed an interplanar distance between the fringes measuring 0.26 nm, indicative of high-quality crystallinity. To assess the practical applicability of these nanocomposites, their feasibility as photocatalysts was rigorously tested. The degradation efficiency of the Cu-MoS_2 nanocomposite exceeded that of both Cu and MoS_2 alone, attributed to the enhanced specific surface area of the photocatalyst and improved separation efficiency of photogenerated electron-hole pairs resulting from the MoS_2 layer coating on the Cu nanorods. Impressively, the Cu-MoS_2 nanocomposites achieved a dye degradation rate of up to 90% for methylene blue (MB) within just 60minutes, highlighting the extraordinary photocatalytic degradation activity of the Cu-MoS_2 nanocomposites. These findings suggest that the integration of MoS_2 with Cu significantly enhances the efficacy of photocatalytic processes, paving the way for advanced applications in environmental remediation and beyond.

Conflicts of Interest

The authors declare that they have no conflict of interest.

Credit authorship contribution agreement

Arti: Methodology, Investigation, Visualization, Writing – original draft, Writing – review & editing. **Naushad Alam** and **Jamilur R. Ansari:** Supervision, Validation, Project administration, funding acquisition. All the authors have read and discussed the data and agreed to the published version of the manuscript.

Acknowledgments

Arti and **Naushad Alam** gratefully acknowledge the support from LNMU in the form of a Research Fellowship. The authors thank Yonsei University for carrying out TEM/HRTEM characterizations. **Jamilur R. Ansari** is thankful to LIET, Alwar, for the financial support.

References

[1] M. Vasylius, A. Tadžijevas, D. Šapalas, V. Kartašovas, J. Janutėnienė, P. Mažeika, Degradation of Mechanical Properties of A-PET Films after UV Aging, Polymers 15 (2023) 4166. https://doi.org/10.3390/polym15204166.

[2] Y. Xu, Z. Wu, A. Li, N. Chen, J. Rao, Q. Zeng, Nanocellulose Composite Films in Food Packaging Materials: A Review, Polymers 16 (2024) 423. https://doi.org/10.3390/polym16030423.

[3] S. Kapoor, V. Kumar, K.B. Tikoo, B. Chudasama, N. Goel, S. Singhal, Strategically designed reduced graphene oxide based magnetic responsive nanocatalysts for the attenuation of recalcitrant pollutants, Ceram. Int. 46 (2020) 2724–2742. https://doi.org/10.1016/j.ceramint.2019.09.262.

[4] W.J. Chong, S. Shen, Y. Li, A. Trinchi, D. Pejak, I. (Louis) Kyratzis, A. Sola, C. Wen, Additive manufacturing of antibacterial PLA-Coppernanocomposites: Benefits, limitations and open challenges, J. Mater. Sci. Technol. 111 (2022) 120–151. https://doi.org/10.1016/j.jmst.2021.09.039.

[5] S. Roy, H.C. Kim, P.S. Panicker, J.-W. Rhim, J. Kim, Cellulose Nanofiber-Based Nanocomposites Films Reinforced with Zinc Oxide Nanorods and Grapefruit Seed Extract, Nanomaterials 11 (2021) 877. https://doi.org/10.3390/nano11040877.

[6] F.T. Thema, E. Manikandan, M.S. Dhlamini, M. Maaza, Green synthesis of Copper nanoparticles via Agathosma betulina natural extract, Mater. Lett. 161 (2015) 124–127. https://doi.org/10.1016/j.matlet.2015.08.052.

[7] J.R. Ansari, N. Singh, S. Anwar, S. Mohapatra, A. Datta, Silver nanoparticles decorated two dimensional MoS2 nanosheets for enhanced photocatalytic activity, Colloids Surf. Physicochem. Eng. Asp. 635 (2022) 128102. https://doi.org/10.1016/j.colsurfa.2021.128102.

[8] X. Gan, H. Zhao, X. Quan, Two-dimensional MoS2: A promising building block for biosensors, Biosens. Bioelectron. 89 (2017) 56–71. https://doi.org/10.1016/j.bios.2016.03.042.

[9] S. Thakur, P. Bandyopadhyay, S.H. Kim, N.H. Kim, J.H. Lee, Enhanced physical properties of two dimensional MoS2/poly(vinyl alcohol) nanocompositess, Compos. Part Appl. Sci. Manuf. 110 (2018) 284–293. https://doi.org/10.1016/j.compositesa.2018.05.009.

[10] F. Wang, M. Cao, Y. Qin, J. Zhu, L. Wang, Y. Tang, Copper nanoparticle-decorated two-dimensional titanium carbide with enhanced supercapacitive performance, RSC Adv. 6 (2016) 88934–88942. https://doi.org/10.1039/C6RA15384D.

[11] S.R. Gottam, C.-T. Tsai, C.-Y. Li, S.-Y. Chu, Investigation of MoS_2 Nanosheet-Coated Copper Thin Films for Hydrogen Gas Sensing Applications and the Effect of Temperature on the Enhanced Sensor Response, J. Electrochem. Soc. 167 (2020) 087507. https://doi.org/10.1149/1945-7111/ab8f59.

[12] T. Yang, M. Chen, Q. Kong, X. Luo, K. Jiao, Toward DNA electrochemical sensing by free-standing Copper nanosheets grown on 2D thin-layered MoS2, Biosens. Bioelectron. 89 (2017) 538–544. https://doi.org/10.1016/j.bios.2016.03.025.

[13] O. Samy, S. Zeng, M.D. Birowosuto, A. El Moutaouakil, A Review on MoS2 Properties, Synthesis, Sensing Applications and Challenges, Crystals 11 (2021) 355. https://doi.org/10.3390/cryst11040355.

[14] Q. Liang, L. Jiang, J. Zheng, N. Duan, Determination of High Concentration Copper Ions Based on Ultraviolet—Visible Spectroscopy Combined with Partial Least Squares Regression Analysis, Processes 12 (2024) 1408. https://doi.org/10.3390/pr12071408.

[15] N. Ben Halima, Poly(vinyl alcohol): review of its promising applications and insights into

biodegradation, RSC Adv. 6 (2016) 39823–39832. https://doi.org/10.1039/C6RA05742J.

[16] H.S. Nalwa, A review of molybdenum disulfide (MoS_2) based photodetectors: from ultra-broadband, self-powered to flexible devices, RSC Adv. 10 (2020) 30529–30602. https://doi.org/10.1039/D0RA03183F.

[17] J. Kabel, S. Sharma, A. Acharya, D. Zhang, Y.K. Yap, Molybdenum Disulfide Quantum Dots: Properties, Synthesis, and Applications, C 7 (2021) 45. https://doi.org/10.3390/c7020045.

[18] J. Ma, Y. Li, X. Yin, Y. Xu, J. Yue, J. Bao, T. Zhou, Poly(vinyl alcohol)/graphene oxide nanocomposites prepared by in situ polymerization with enhanced mechanical properties and water vapor barrier properties, RSC Adv. 6 (2016) 49448–49458. https://doi.org/10.1039/C6RA08760D.

[19] C. Wu, K. Liu, Y. Li, L. Wang, S. Guo, Y. Sun, F. Zhang, G. Shao, P. Zhang, Dual-Modified Hollow Spherical Shell MoS_2 [at]TiO_2 /TiN Composites for Photocatalytic Hydrogen Production, Energy Technol. 10 (2022) 2100265. https://doi.org/10.1002/ente.202100265.

[20] O. Samy, S. Zeng, M.D. Birowosuto, A. El Moutaouakil, A Review on MoS2 Properties, Synthesis, Sensing Applications and Challenges, Crystals 11 (2021) 355. https://doi.org/10.3390/cryst11040355.

[21] M. Donarelli, L. Ottaviano, 2D Materials for Gas Sensing Applications: A Review on Graphene Oxide, MoS2, WS2 and Phosphorene, Sensors 18 (2018) 3638. https://doi.org/10.3390/s18113638.

[22] O. Samy, S. Zeng, M.D. Birowosuto, A. El Moutaouakil, A Review on MoS2 Properties, Synthesis, Sensing Applications and Challenges, Crystals 11 (2021) 355. https://doi.org/10.3390/cryst11040355.

[23] Y. Wang, F. Chen, X. Ye, T. Wu, K. Wu, C. Li, Photoelectrochemical immunosensing of tetrabromobisphenol A based on the enhanced effect of dodecahedral gold nanocrystals/MoS2 nanosheets, Sens. Actuators B Chem. 245 (2017) 205–212. https://doi.org/10.1016/j.snb.2017.01.140.

[24] S. Roy, R. Priyadarshi, J.-W. Rhim, Development of Multifunctional Pullulan/Chitosan-Based Composite Films Reinforced with Copper Nanoparticles and Propolis for Meat Packaging Applications, Foods 10 (2021) 2789. https://doi.org/10.3390/foods10112789.

[25] P. Berwal, S. Rani, S. Sihag, P. Singh, R. Dahiya, A. Kumar, A. Sanger, A.K. Mishra, V. Kumar, Hydrothermal synthesis of MoS2 with tunable band gap for future nano-electronic devices, Inorg. Chem. Commun. 159 (2024) 111833. https://doi.org/10.1016/j.inoche.2023.111833.

[26] F. Chekin, R. Boukherroub, S. Szunerits, MoS2/reduced graphene oxide nanocomposites for sensitive sensing of cysteamine in presence of uric acid in human plasma, Mater. Sci. Eng. C 73 (2017) 627–632. https://doi.org/10.1016/j.msec.2016.12.102.

[27] H. Sun, J. Chao, X. Zuo, S. Su, X. Liu, L. Yuwen, C. Fan, L. Wang, Gold nanoparticle-decorated MoS2 nanosheets for simultaneous detection of ascorbic acid, dopamine and uric acid, RSC Adv. 4 (2014) 27625. https://doi.org/10.1039/c4ra04046e.

[28] A. Sinha, Dhanjai, B. Tan, Y. Huang, H. Zhao, X. Dang, J. Chen, R. Jain, MoS2 nanostructures for electrochemical sensing of multidisciplinary targets: A review, TrAC Trends Anal. Chem. 102 (2018) 75–90. https://doi.org/10.1016/j.trac.2018.01.008.

[29] M. Choi, J. Lim, J. Yang, Synergistic role of MoS2 in gelation-induced fabrication of graphene oxide films, Sci. Rep. 14 (2024) 12159. https://doi.org/10.1038/s41598-024-62146-4.

[30] G. Deme, A. Belay, D.M. Andoshe, G. Barsisa, D. Tsegaye, S. Tiruneh, C. Seboka, Effect of Hydrothermal Reaction Temperature on Fluorescent Properties of Carbon Quantum Dots Synthesized from Lemon Juice for Adsorption Applications, J. Nanomater. 2023 (2023) 1–10. https://doi.org/10.1155/2023/1701496.

[31] N.U.M. Nizam, M.M. Hanafiah, E. Mahmoudi, A.W. Mohammad, Synthesis of highly fluorescent carbon quantum dots from rubber seed shells for the adsorption and photocatalytic degradation of dyes, Sci. Rep. 13 (2023) 12777. https://doi.org/10.1038/s41598-023-40069-w.

[32] S. Bhandari, D. Mondal, S.K. Nataraj, R.G. Balakrishna, Biomolecule-derived quantum dots for sustainable optoelectronics, Nanoscale Adv. 1 (2019) 913–936. https://doi.org/10.1039/C8NA00332G.

[33] R. Wang, K.-Q. Lu, Z.-R. Tang, Y.-J. Xu, Recent progress in carbon quantum dots: synthesis, properties and applications in photocatalysis, J. Mater. Chem. A 5 (2017) 3717–3734. https://doi.org/10.1039/C6TA08660H.